American Journal of Modern Physics and Application
2018; 5(1): 9-23
http://www.openscienceonline.com/journal/ajmpa

Exact In-Plane Natural Frequencies in Purely Radial Modes and Corresponding Critical Speeds of Functionally Graded (FG) Non-Uniform Disks

Vebil Yıldırım

Mechanical Engineering Department, Cukurova University, Adana, Turkey

Email address

vebil@cu.edu.tr

To cite this article

Vebil Yıldırım. Exact In-Plane Natural Frequencies in Purely Radial Modes and Corresponding Critical Speeds of Functionally Graded (FG) Non-Uniform Disks. *American Journal of Modern Physics and Application*. Vol. 5, No. 1, 2018, pp. 9-23.

Received: March 24, 2018; **Accepted**: March 30, 2018; **Published**: April 27, 2018

Abstract

This paper analytically tackles with the axisymmetric in-plane purely radial free vibrations of hollow continuously hyperbolically varying thickness disks made of functionally power-law graded materials having identical inhomogeneity indexes for both elasticity modulus and the material density. The equation of motion which is in the form of a linear second-order homogeneous Bessel's ordinary differential equation with constant coefficients is derived by using the linear elasticity theory under plane stress assumption. For practical use, three boundary conditions are chosen as a stress-free annulus, and disks mounted on a rigid shaft at the inner surface with/without rigid casing at the outer surface. For those constraints, characteristic free vibration equations are offered in closed forms. The present frequencies are validated with the results for uniform isotropic and homogeneous disks in the open literature. The influences of boundary conditions, the disk profile parameters, the inhomogeneity indexes, and the aspect ratios (inner radius/outer radius) on the pure radial frequencies are all investigated. Results are reported in both graphical and tabular forms. It was mainly observed that the variation of the vibrational parameters have much more influence over the fundamental frequencies which strictly correspond to the critical rotational speeds of rotating disks. The extensive literature survey showed that there is no such reported analytical solutions to the problem in question. In this regard, the present analytical solutions deserve to be appreciated although such an additional restriction for the inhomogeneity indexes of both the elasticity modulus and the density have been used in the formulation.

Keywords

In-Plane Free Vibration, Critical Rotational Speeds, Variable Thickness Disk, Functionally Graded, Axisymmetric

1. Introduction

There are numerous studies, some of whom were reviewed by Leissa [1-5], and Swaminathan et al. [6], concerning the free vibration of circular/annular plates or disks with uniform or varying thicknesses in the available literature. Most of those of studies dealt with uniform solid/annular disks made of an isotropic and homogeneous material [7-21]. Brunelle [7] first reported the existence of a static inertia-elastic instability of rotating beams and disks. Ambati et al. [8] worked theoretically and experimentally on in-plane vibrations of solid disks and rings to evaluate the natural frequencies and mode shapes for general case of annular configuration. They also classified the disk modes by the number of nodal circles and nodal diameters such as pure tension, pure radial, finite, flexural, shear wave and plate wave modes. Civalek [13] studied the out-of-plane free vibration analysis of circular and annular plates based on the discrete singular convolution method. Bashmal et al. [16] dealt with the exact in-plane free vibration of an elastic and isotropic disks under combinations of different boundary conditions on the basis of the two-dimensional linear plane stress theory of elasticity. The exact solution was presented in terms of Bessel functions. However, they did not presented the purely radial natural frequencies which corresponds to zero nodal circles (n=0) with even subsystem. In another study, Bashmal et al. [17] discussed in details the mode couplings in in-plane free vibration of circular plates. Bashmal et al. [17] revealed that, for axisymmetric modes, (n=0), the modes are purely in radial or purely circumferential. The even subsystem would yield axisymmetric radial modes, while the odd subsystem gives the axisymmetric circumferential modes [17]. The node (m, n)=(0, 0) may also show purely radial mode or purely circumferential mode [17] under classical boundary conditions. Bashmal et al. [17] also stated that, for a disk with non-uniform boundary conditions, nature of coupling between the modes would differ from those observed under classical boundary conditions. Carrera et al. [18] extended Carrera's unified formulation to perform free-vibrational analyses of rotating structures. Squarcella [19] presented a numerical method to predict the burst speed based on the finite element solutions taking into account the spin-softening effect which leads to instability and therefore to the burst speed of the disk. Mercan et al. [21] investigated free vibration analysis of annular plates by using two different numerical methods such as differential quadrature and discrete singular convolution methods.

As for the free vibration of variable thickness disks made of a homogeneous and isotropic materials, References [22-39] may be cited. From those, Sato and Shimizu [23] employed the transfer matrix method, Shahab [24] exploited the finite element method, and Wang [29] exercised generalized power series solution. Singh and Saxsena [26] studied axisymmetric vibration of a circular plate with exponential variation. Kang and Leissa [32] and Kang [35] considered 3-D vibration analysis of variable thickness disks. Salmane and Lakis [32], Eisenberger and Jabereen [34], and Duan et al. [37] worked on the bending vibrations of variable thickness disks. Bhardwaj et al. [39] studied asymmetric vibration of polar orthotropic annular circular plates of quadratically varying thickness resting on Winkler elastic foundation by using boundary characteristic orthonormal polynomials in Rayleigh-Ritz method.

In-plane and out-of-plane free vibrations of solid/hollow uniform disks made of functionally graded materials (FGM) were investigated in References [40-59]. Among those, Efraim and Eisenberger [42] solved exactly the bending equations of motion for various combinations of boundary conditions for the first time based on the first order shear deformation theory and the exact element method. Efraim and Eisenberger [42] considered linear, quadratically concave, and quadratically convex forms as types of variation of the plate thickness. Keleş and Tutuncu [50] analytically performed axisymmetric free and forced vibration analyses of power-law graded hollow cylinders (or disks) and spheres. Çallıoğlu et al. [54] studied the transverse free vibration of radially functionally graded annular disk with hyperbolic geometry. Torabi and Ansari [57] studied the nonlinear free vibration of carbon nanotube (CNT) reinforced composite annular plates under thermal loading based on the asymmetric formulation due to the fact that the initial thermal loading can change the axisymmetric vibration behavior of annular plates. Based on the two-dimensional linear elastic theory, Yang et al. [58] presented an analysis of the in-plane free vibration of the circular and annular functionally graded uniform disks by a meshfree boundary-domain integral equation method. The material properties of the disks with combinations of free and clamped boundary conditions were assumed to vary in the radial direction obeying an exponential law in Yang et al.'s study [58]. Based on the first shear deformation theory and employing the modified couple stress theory, Mahinzare et al. [59] formulated the free vibration of a rotating circular nanoplate made of two directional functionally power-law graded piezo materials and solved the governing equations with the help of the differential quadrature method.

As the literature suggests, the in-plane free vibration analyses of circular disks [7-11, 15-17, 19, 48, 50, 58] have gained much less attention from the investigators although they have important significance in various practical problems such as the vibration of railway wheels, aero-engine disks, disk brakes, and hard disk drives contributing to noise and structural vibration. Among these works only References [48, 50, 58] are related to the uniform thickness disks made of functionally graded materials. In conclusion, no reported in-plane purely radial frequencies of variable thickness disks made of radially functionally graded material were found in the open literature. This has motivated the author.

As explained in Abstract, the present study is limited to the exact radial free vibration of continuously hyperbolically varying thickness disks made of power-law graded isotropic materials. The substance aim of the present study is to have a general idea for the vibrational characteristics of such structures. To achieve this, the equation of motion is first derived on the basis of the linear elasticity field equations under axisymmetric plane stress assumptions. Frequency equation is then obtained in an explicit form for three boundary conditions. The influences of the boundary conditions, inhomogeneity indexes, profile parameters, and (inner radius/outer radius) ratios on the radial frequencies are all investigated. Since there is no reported frequencies which fall into the realm of purely radial free vibrations of FGM disks with varying thickness, the present analytical solutions have practical importance although such an additional restriction made for the inhomogeneity indexes of both the elasticity modulus and the density have been used in the formulation.

2. Theory

By using the prime symbol for the derivative, the strain-displacement relations in polar coordinates, under axisymmetric plain stress and small deformations assumptions, are given by

$$\varepsilon_r(r) = u_r\,'(r), \quad \varepsilon_\theta(r) = \frac{u_r(r)}{r} \tag{1}$$

where the radial unit strain and the tangential unit strain are indicated by $\varepsilon_r(r)$ and $\varepsilon_\theta(r)$, respectively. In Eqn. (1), the radial displacement is represented by $u_r(r)$. If $\sigma_r(r)$ and

$\sigma_\theta(r)$ suggest the radial stress and the hoop stress, respectively, then the stress-strain relations, namely Hooke's law, for a disk made of an isotropic and homogeneous linear elastic material are defined as follows

$$\sigma_r(r) = \frac{E(r)}{(1-\nu^2)}\varepsilon_r(r) + \frac{E(r)\nu}{(1-\nu^2)}\varepsilon_\theta(r) = C_{11}(r)\varepsilon_r(r) + C_{12}(r)\varepsilon_\theta(r) \tag{2}$$

$$\sigma_\theta(r) = \frac{E(r)\nu}{(1-\nu^2)}\varepsilon_r(r) + \frac{E(r)}{(1-\nu^2)}\varepsilon_\theta(r) = C_{12}(r)\varepsilon_r(r) + C_{11}(r)\varepsilon_\theta(r) \tag{3}$$

where $E(r)$ is Young's modulus and ν is Poisson's ratio. For an isotropic but non-homogeneous functionally graded (FG) material, the material grading rule in the radial direction is assumed to be observed the following simple power rule

$$E(r) = E_b(\frac{r}{b})^\eta, \; \rho(r) = \rho_b(\frac{r}{b})^\eta \tag{4}$$

where $\rho(r)$ is the material density; a and b are the inner and outer radii of the disk, respectively (Figure 1). The material inhomogeneity index is denoted by η. E_b and ρ_b are the reference values of the mixture of the material at the outer surface. Poisson's ratio of the graded material is assumed to be constant along the radial direction as in the most of studies in the related realm. In Eqn. (4) those properties do not completely corresponds to a physical material since both Young's modulus and density are assumed to have the same inhomogeneity index. To get an analytical solution to the problem, as seen later, taking both inhomogeneity indexes as if they are identical is going to be inevitable otherwise it is not possible to find a closed-form solution by using the other choices which requires exactly numerical solution techniques.

To consider the continuously radial variation of the thickness of the disk, the following hyperbolic profile is supposed.

$$h(r) = h_o(\frac{r}{a})^m \tag{5}$$

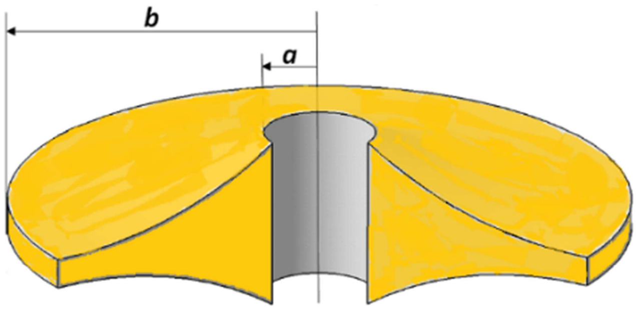

Convergent hyperbolic profile ($m<0$)

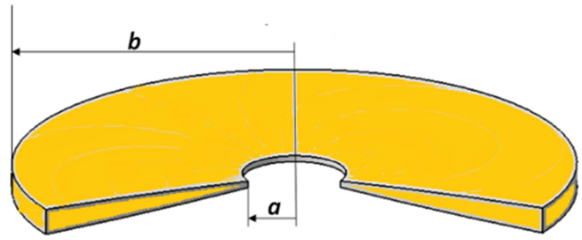

Divergent hyperbolic profile ($m>0$)

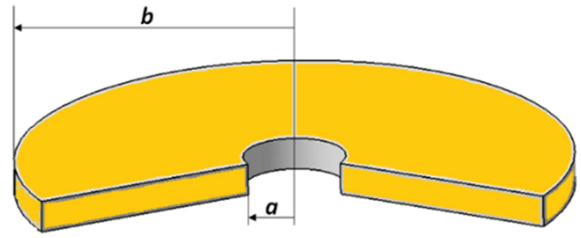

Uniform profile ($m=0$)

Figure 1. *Geometry of a hyperbolic disk.*

where m is the thickness or profile parameter, whose positive values $(m>0)$ result in divergent disk profiles. To get convergent disk profiles, one needs to use negative values of the thickness parameter $(m<0)$. Uniform disk profiles correspond to $m=0$ (*Figure* 1) while $m=1$ gives a linear disk profile with positive slope (a linearly increasing divergent profile).

When the body forces are ignored, the equation of motion in the radial direction is written as follows

$$\frac{1}{rh(r)}\frac{\partial}{\partial r}\left(rh(r)\sigma_r(r)\right) - \frac{\sigma_\theta(r)}{r} = \rho(r)\frac{\partial^2 u_r(r)}{\partial t^2} \tag{6}$$

where t is the time. Substitution Eqns. (1)-(3) together with Eqns. (4)-(5) into Eqn. (6) gives

$$\left(\begin{array}{l} \dfrac{\partial^2 u_r}{\partial r^2} + \left(\dfrac{1+\eta+m}{r}\right)\dfrac{\partial u_r}{\partial r} \\ -\dfrac{\left(1-(\eta+m)\dfrac{C_{12}(r)}{C_{11}(r)}\right)}{r^2}u_r \end{array}\right) = -\left(\frac{\rho(r)}{C_{11}(r)}\right)\frac{\partial^2 u_r}{\partial t^2} \tag{7}$$

By assuming a harmonic motion with an angular velocity $\omega\ (rad/s)$, $u_r(r,t) = u_r^*(r)\, e^{i\omega t}$, the equation of motion will be in the form of

$$\frac{d^2u_r^*}{dr^2} + \left(\frac{1+\eta+m}{r}\right)\frac{du_r^*}{dr} - \left(\frac{1-\nu(\eta+m)}{r^2} + \Omega^2\right)u_r^* = 0 \tag{8}$$

where

$$\Omega = \sqrt{\frac{\rho(r)}{C_{11}(r)}}\omega = \sqrt{\frac{(1-\nu^2)\rho_b}{E_b}}\omega = \frac{\gamma}{a} \tag{9}$$

and γ is the dimensionless natural frequency. The solution to this equation is going to be in the form of [60]

$$u_r^*(r) = r^{\frac{1}{2}(-\eta-m)}\left(B_1 J_{\xi/2}(r\Omega) + B_2 Y_{\xi/2}(r\Omega)\right) \tag{10}$$

where

$$\xi = \sqrt{4+(m+\eta)(m+\eta-4\nu)} \tag{11}$$

B_1 and B_2 are arbitrary constants, $J_{\xi/2}(r\Omega)$ and $Y_{\xi/2}(r\Omega)$ stand for Bessel's functions of the first and second kind of order $\xi/2$, respectively. The first derivative of the solution of the radial displacement, $u_r^*(r)$, and the radial stress, $\sigma_r^*(r)$, may be derived in terms of unknown constants, B_1 and B_2, as follows

$$\frac{du_r^*}{dr}(r) = \frac{1}{2}(-\eta-m))r^{\frac{-\eta-m-1}{2}}\left(B_1 J_{\xi/2}(r\Omega) + B_2 Y_{\xi/2}(r\Omega)\right) + r^{\frac{-\eta-m}{2}}\left(\begin{array}{l} \frac{1}{2}B_1\Omega\left(J_{\frac{\xi}{2}-1}(r\Omega) - J_{\frac{\xi}{2}+1}(r\Omega)\right) \\ +\frac{1}{2}B_2\Omega\left(Y_{\frac{\xi}{2}-1}(r\Omega) - Y_{\frac{\xi}{2}+1}(r\Omega)\right)\end{array}\right) \tag{12}$$

$$\sigma_r^*(r) = \frac{E_b(\frac{r}{b})^{\eta} r^{\frac{-\eta-m-2}{2}}}{2(1-\nu^2)}\left(\begin{array}{l} -B_1(\eta+m-2\nu)J_{\xi/2}(r\Omega) \\ +B_1 r\Omega J_{\frac{\xi-2}{2}}(r\Omega) \\ -B_1 r\Omega J_{\frac{\xi+2}{2}}(r\Omega) \\ -B_2(\eta+m-2\nu)Y_{\xi/2}(r\Omega) \\ +B_2 r\Omega Y_{\frac{\xi-2}{2}}(r\Omega) \\ -B_2 r\Omega Y_{\frac{\xi+2}{2}}(r\Omega)\end{array}\right) \tag{13}$$

Eqns. (10) and (13) are to be used for application of the boundary conditions defined at inner and outer surfaces. As is well known, the radial displacement vanishes, $u_r^* = 0$, at the fixed surface while the radial stress becomes zero, $\sigma_r^* = 0$, at the free surface. For instance, if fixed-free boundaries are studied then one may get

$$\begin{Bmatrix} u_r^*(a) \\ \sigma_r^*(b) \end{Bmatrix} = \mathrm{A}\begin{Bmatrix} B_1 \\ B_2 \end{Bmatrix} = \begin{Bmatrix} 0 \\ 0 \end{Bmatrix} \tag{14}$$

The natural frequencies which make the determinant of the characteristic coefficient matrix zero, $|\mathrm{A}|$, give non-trivial solutions. Elements of the coefficient matrices are established in an explicit form, for the stress-free boundary conditions, $\sigma_r^*(a) = \sigma_r^*(b) = 0$ (FF), as follows

$$A_{1,1}^{FF} = \frac{E_b(\frac{a}{b})^{\eta} a^{\frac{-\eta-m-2}{2}}}{2(1-\nu^2)}\left(\begin{array}{l} a\Omega J_{\frac{\xi-2}{2}}(a\Omega) - a\Omega J_{\frac{\xi+2}{2}}(a\Omega) \\ -(\eta+m-2\nu)J_{\xi/2}(a\Omega)\end{array}\right) \tag{15}$$

$$A_{1,2}^{FF} = \frac{E_b(\frac{a}{b})^{\eta} a^{\frac{-\eta-m-2}{2}}}{2(1-\nu^2)}\left(\begin{array}{l} a\Omega Y_{\frac{\xi-2}{2}}(a\Omega) - a\Omega Y_{\frac{\xi+2}{2}}(a\Omega) \\ -(\eta+m-2\nu)Y_{\xi/2}(a\Omega)\end{array}\right) \tag{16}$$

$$A_{2,1}^{FF} = \frac{E_b b^{\frac{-\eta-m-2}{2}}}{2(1-\nu^2)}\left(\begin{array}{l} b\Omega J_{\frac{\xi-2}{2}}(b\Omega) - b\Omega J_{\frac{\xi+2}{2}}(b\Omega) \\ -(\eta+m-2\nu)J_{\xi/2}(b\Omega)\end{array}\right) \tag{17}$$

$$A_{2,2}^{FF} = \frac{E_b b^{\frac{-\eta-m-2}{2}}}{2(1-\nu^2)}\left(\begin{array}{l} b\Omega Y_{\frac{\xi-2}{2}}(b\Omega) - b\Omega Y_{\frac{\xi+2}{2}}(b\Omega) \\ -(\eta+m-2\nu)Y_{\xi/2}(b\Omega)\end{array}\right) \tag{18}$$

for a disk mounted on a rigid shaft at its center, $u_r^*(a) = \sigma_r^*(b) = 0$ (CF), as

$$A_{1,1}^{CF} = a^{\frac{-\eta-m}{2}} J_{\xi/2}(a\Omega), \quad A_{1,2}^{CF} = a^{\frac{-\eta-m}{2}} Y_{\xi/2}(a\Omega) \tag{19}$$

$$A_{2,1}^{CF} = \frac{E_b b^{\frac{-\eta-m-2}{2}}}{2(1-\nu^2)}\left(\begin{array}{l} b\Omega J_{\frac{\xi-2}{2}}(b\Omega) - b\Omega J_{\frac{\xi+2}{2}}(b\Omega) \\ -(\eta+m-2\nu)J_{\xi/2}(b\Omega)\end{array}\right) \tag{20}$$

$$A_{2,2}^{CF} = \frac{E_b b^{\frac{-\eta-m-2}{2}}}{2(1-\nu^2)}\left(\begin{array}{l} b\Omega Y_{\frac{\xi-2}{2}}(b\Omega) - b\Omega Y_{\frac{\xi+2}{2}}(b\Omega) \\ -(\eta+m-2\nu)Y_{\xi/2}(b\Omega)\end{array}\right) \tag{21}$$

for a disk mounted on a rigid shaft at its center, and having a rigid case at its outer surface, $u_r^*(a) = u_r^*(b) = 0$ (CC), as

$$A_{1,1}^{CC} = a^{\frac{-\eta-m}{2}} J_{\xi/2}(a\Omega), \quad A_{1,2}^{CC} = a^{\frac{-\eta-m}{2}} Y_{\xi/2}(a\Omega) \tag{22}$$

$$A_{2,1}^{CC} = b^{\frac{-\eta-m}{2}} J_{\xi/2}(b\Omega), \quad A_{2,2}^{CC} = b^{\frac{-\eta-m}{2}} Y_{\xi/2}(b\Omega) \tag{23}$$

3. Verification of the Results

As a first example a hollow disk with $a = 2.5cm$, $\nu = 0.33$ is considered [8]. Ambati et al. [8] studied traction free boundaries with $a/b = 0.5$ and $a/b = 0.9$ for fundamental frequencies. They also gave the fundamental frequency as $71.405\ kHz$ for a solid disk having the same properties. Table 1 clearly shows that present results are in a good harmony with the open literature. As stated before, Ambati et al. [8] classified frequency modes therefore the pure radial modes were clearly defined in the examples in this Reference.

The second example is also taken from the Reference [8]. In this example, Ambati et al. [8] presented dimensionless frequencies belonging to the second and third modes for a free-free circular uniform annulus of $a = 2.5cm$. They did not presented the fundamental purely radial frequency. In Reference [8], dimensionless frequency, K_p, is defined by

$$K_p = \frac{\omega b}{5421} = \gamma \frac{b}{a} = \Omega\ b \qquad (24)$$

Table 1. *Dimensional fundamental frequencies (kHz) of the first example* $(C_p = E/(\rho\sqrt{1-\nu^2}) = 5421\ m/s)$.

	a/b=0.1	*a/b=0.9*
Present	45.3003	34.3292
Ambati et al. [8]	45.427	34.331

Table 2. *The dimensionless frequencies,* K_p*, for the second example.*

	a/b				
	0.1	**0.3**	**0.5**	**0.7**	**0.9**
ν	*First mode* (Present)				
0	1.80347	1.58206	1.35467	1.18236	1.05312
0.1	1.86893	1.60737	1.35838	1.17892	1.04803
0.2	1.92678	1.61816	1.34824	1.16338	1.03222
0.3	1.97658	1.61259	1.32325	1.13508	1.00517
0.4	2.01709	1.5878	1.28174	1.09288	0.96591
0.5	2.04565	1.53945	1.22118	1.03489	0.91287
ν	*Second mode* (Present)				
0	5.13714	5.1374	6.56494	10.5918	31.4469
0.1	5.11145	5.0828	6.53526	10.5784	31.4433
0.2	5.07485	5.0235	6.50488	10.5649	31.4398
0.3	5.02334	4.9595	6.47384	10.5513	31.4363
0.4	4.95092	4.8909	6.44224	10.5377	31.4328
0.5	4.84846	4.8179	6.41014	10.524	31.4292
ν	*Second mode* (Ambati et al. [8])				
0	5.1372	5.1373	6.5649	10.592	31.446
0.1	5.1113	5.0828	6.5353	10.578	31.443
0.2	5.0747	5.0235	6.5049	10.565	31.440
0.3	5.0232	4.9596	6.4738	10.551	31.436
0.4	4.9507	4.8909	6.4422	10.537	31.433
0.5	4.8482	4.8179	6.4101	10.524	31.429
ν	*Third mode* (Present)				
0	8.19916	9.3083	12.7064	21.0037	62.8473
0.1	8.13646	9.2732	12.6907	20.9969	62.8456
0.2	8.06097	9.2373	12.675	20.9901	62.8438
0.3	7.97017	9.2006	12.6591	20.9833	62.842
0.4	7.86136	9.1633	12.6432	20.9764	62.8402
0.5	7.73211	9.1254	12.6272	20.9697	62.8384
ν	*Third mode* (Ambati et al. [8])				
0	8.1992	9.3083	12.707	21.003	62.842
0.1	8.1365	9.2732	12.691	20.997	62.846
0.2	8.0610	9.2373	12.675	20.990	62.844
0.3	7.9702	9.2006	12.659	20.983	62.842
0.4	7.8613	9.1633	12.643	20.976	62.840
0.5	7.7321	9.1254	12.627	20.970	62.839

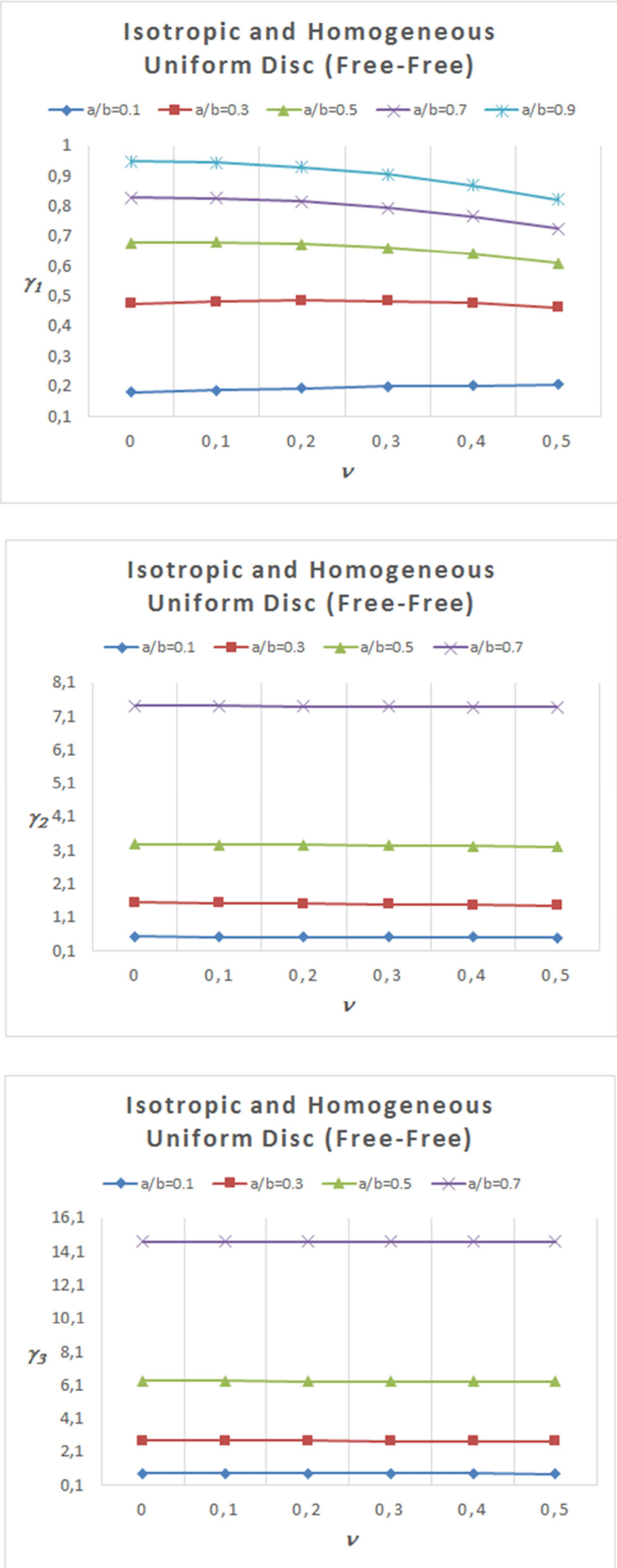

Figure 2. *Variation of the present first three dimensionless radial frequencies with Poisson's and aspect ratios for the second example.*

In this example Ambati et al. [8] studied the variation of the dimensionless natural frequencies with Poisson's ratio and aspect ratios. This is shown in Table 2. This comparison given in Table 2 shows a perfect agreement between the results.

Variation of the present first three dimensionless radial frequencies with Poisson's and aspect ratios for the second example is also illustrated in *Figure* 2. Both Table 2 and *Figure* 2 suggest that

1. There is an increase in the frequencies with increasing (a/b) ratios for all values of Poisson's ratios. That is when the thickness decreases, as a consequence the frequencies increase.
2. As Poisson's ratio increases, the second and third natural frequencies decreases with small amounts for all aspect ratios. However, different responses may be observed for the fundamental frequency. For example, for $a/b=0.1$, as Poisson's ratio increases, consequently frequencies increase. For $0.1<a/b<0.5$, the frequencies first increase, then decrease with increasing Poisson's ratio. For $a/b>0.5$, the frequencies decrease with increasing Poisson's ratio.

As a final test example, a uniform disk of $E=207.6\ GPa$ $\rho=7456\ \ kg/m^3$ $\nu=0.3$ $b=1\,m$ is studied. The results are presented in Table 3. Table 3 verifies that the present results are in a good harmony with the reported Brunelle's analytical [7], Squarcella et al.'s analytical [19], Irie et al.'s numeric based on the transfer matrix method [9], Basmal et al.'s analytical [17] and numerical based on the finite element analysis with the aid of Ansys [17] solutions for clamped-free supported uniform disks made of an isotropic and homogeneous material.

Variation of the present first three dimensionless radial frequencies with aspect ratios for the third example under FF and CF boundary conditions are illustrated in Figure 3. For FF boundary conditions, the fundamental frequency decreases with increasing aspect ratios (Table 3 and Figure 3). However, the converse is true for both CF and CC boundary conditions.

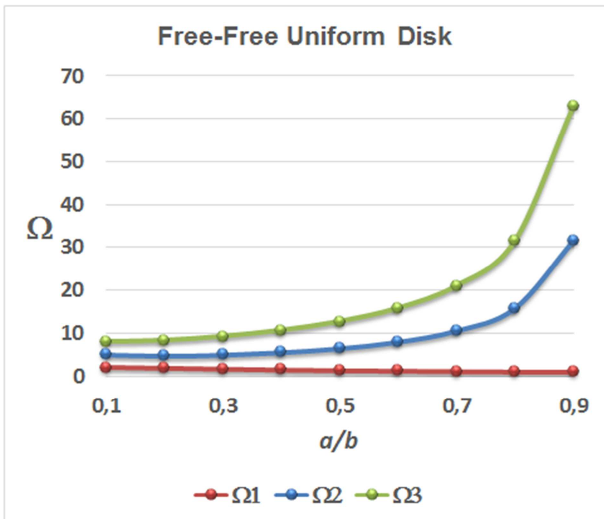

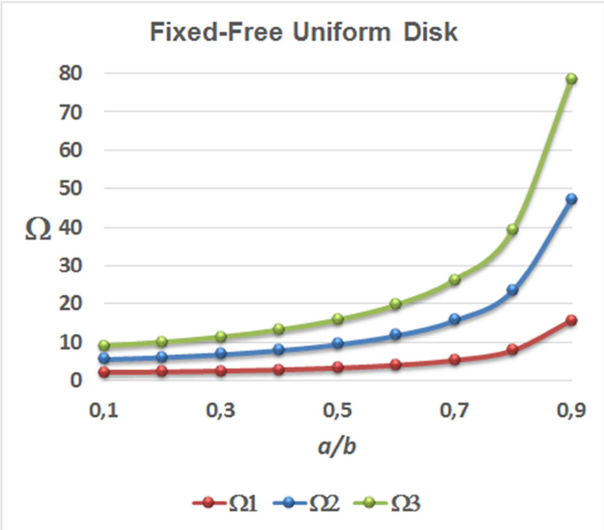

***Figure 3.** Variation of the present first three dimensionless radial frequencies with aspect ratios for the third example under FF and CF boundary conditions.*

4. Numerical Examples for FGM Hyperbolic Disks

In this section a FGM disk of $\nu = 0.3$ is considered. The functionally graded material is taken to be a hypothetical one exhibiting significant inhomogeneity $(-3 \le \eta \le 3)$.

Figure 4 illustrates some determinant-dimensionless frequency curves with respect to the boundary conditions in the interval of $(0 < \gamma \le 10)$. As stated before, $\gamma-$ intercepts are referred to as natural frequencies.

Variation of the first six natural frequencies with the profile parameter, inhomogeneity index, and boundary conditions of a FGM disk with $a/b = 0.1$ are seen in Tables 4-6 for free-free, fixed-free, and fixed-fixed boundary conditions. Tables 7 and 8 show the similar comparisons for $a/b = 0.5$ and $a/b = 0.9$ for the first three natural frequencies. Due to space constraints, In Tables 7-8, some particular values of the inhomogeneity index such as $\eta = -3, 0, 3$ are given.

From Tables 4-6, an interesting result that a variable thickness FGM disk having the same sum for the inhomogeneity index and thickness parameter exhibits the same natural frequencies is recognized. For example the results for $\eta = -3$, and $m = 0$ will be identical with the frequencies for $\eta = -2$ and $m = -1$. Similar observation may be given for different inhomogeneity index and profile parameter. This physically means that the effective properties for two cases along the radial coordinate are the same. This may be used in optimization problems of such springs.

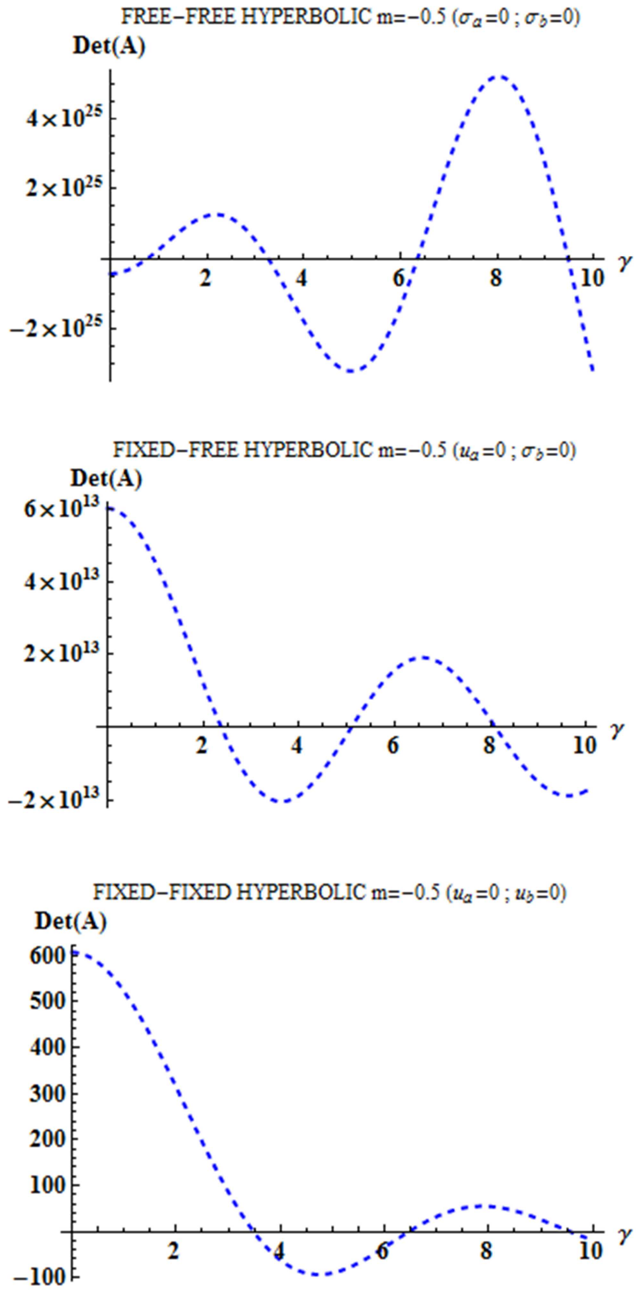

***Figure 4.** The determinant-dimensionless frequency curves for some examples in the interval of* $(0 < \gamma \le 10)$ $(a/b = 0.5,\ m = -0.5,\ \eta = -3)$

To be able to clearly see the expected variations of the fundamental dimensionless frequencies, viz., dimensionless rotational critical speeds with the profile parameter, inhomogeneity index, boundary conditions and aspect ratios, Figure 5 is presented. For free-free and fixed-free boundary conditions, and for all aspect ratios, a decrease is observed in the fundamental frequencies for all inhomogeneity indexes when the profile parameter increases. However this response is different for fixed-fixed boundaries. As the thickness parameter increases there will be a decrease in the fundamental frequencies for negative inhomogeneity indexes while there is an increase for positive inhomogeneity indexes.

5. Conclusions

In the present study, the free vibration behavior of a hollow power-law graded disk with radially continuously varying thickness is studied analytically. Frequency equations are offered in closed forms for three different boundary conditions. An extensive parametric study is performed to understand the variations of natural frequencies with vibrational parameters. The following general conclusions are reached from the present examinations:

1. Fixed-fixed boundaries give the highest frequencies while free-free ones present the smallest.
2. As the profile parameter increases, fundamental frequencies are all decrease except for fixed-fixed boundaries with positive inhomogeneity indexes.
3. As the inhomogeneity indexes change from the negative to the positive (from the convergent profiles to the divergent profiles), fundamental frequencies considerable decrease for all profile parameters except for fixed-fixed boundaries with positive inhomogeneity indexes.
4. Convergent profiles may withstand much higher critical rotational speeds.
5. The fundamental frequencies are mostly affected from the variation of vibrational parameters.
6. For higher modes, from Tables 4-8, frequencies decrease with increasing profile parameter for negative inhomogeneity indexes under all boundary conditions. However different responses are observed for positive inhomogeneity indexes. The similar may be observed for *a/b=0.5* and *a/b=0.9*.

It may be noted that, one may be confronted some numerical difficulties when searching some frequencies if he use all the vibrational parameters as integer numbers. To overcome this difficulty, it may be helpful to use at least one real number instead integer such as m = 1.000000001 for any of parameter when facing with this kind of problems.

Table 3. *Dimensionless purely radial frequencies of the third text example.*

		(CF)						FF	CC
a/b		**[7]**	**[19]**	**[9] (Numeric)**	**[17] (Analytic)**	**[17] (FE)**	**Present**	**Present**	**Present**
0.1	Ω_1	2.088	2.088	--	--	--	2.08794	1.97658	3.94094
	Ω_2	--	--	--	--	--	5.59161	5.02334	7.33057
	Ω_3	--	--	--	--	--	9.01126	7.97017	10.7484
0.2	Ω_1	--	--	2.204	2.2040	2.2039	2.20393	1.80147	4.23575
	Ω_2	--	--	--	--	--	6.0941	4.7481	8.05536
	Ω_3	--	--	--	--	--	9.96156	8.26044	11.9266
0.3	Ω_1	2.404	2.404	--	--	--	2.4043	1.61259	4.70578
	Ω_2	--	--	--	--	--	6.85178	4.95955	9.10423
	Ω_3	--	--	--	--	--	11.2998	9.20061	13.5532
0.4	Ω_1	--	--	--	--	--	2.71346	1.45213	5.39118
	Ω_2	--	--	--	--	--	7.92203	5.52945	10.5577
	Ω_3	--	--	--	--	--	13.134	10.6128	15.7665
0.5	Ω_1	3.183	3.183	--	--	--	3.18342	1.32325	6.39316
	Ω_2	--	--	--	--	--	9.45827	6.47384	12.6247
	Ω_3	--	--	--	--	--	15.7294	12.6591	18.8889
0.6	Ω_1	--	--	--	--	--	3.92372	1.21966	7.93009
	Ω_2	--	--	--	--	--	11.79	7.97884	15.7473
	Ω_3	--	--	--	--	--	19.641	15.7694	23.5883
07	Ω_1	5.194	5.193	--	--	--	5.19439	1.13508	10.522
	Ω_2	--	--	--	--	--	15.699	10.5513	20.9694
	Ω_3	--	--	--	--	--	26.1748	20.9833	31.4329
0.8	Ω_1	--	--	--	--	--	7.77952	1.06473	15.7376
	Ω_2	--	--	--	--	--	23.5391	15.7539	31.4308
	Ω_3	--	--	--	--	--	39.2563	31.4388	47.1338
0.9	Ω_1	15.605	15.604	--	--	--	15.60517	1.00517	31.42916
	Ω_2	--	--	--	--	--	47.0902	31.4363	62.8385
	Ω_3	--	--	--	--	--	78.5196	62.842	94.2522
.95	Ω_1	--	--	--	--	--	31.3004	0.978635	62.8381
	Ω_2	--	--	--	--	--	94.2095	62.8415	125.667
	Ω_3	--	--	--	--	--	157.057	125.669	188.498

Table 4. *Natural frequencies of a free-free FGM disk with* $(a/b = 0.1)$ $(\Omega_i = \gamma_i / 0.1, i = 1,2,..,6)$.

m	**-1**	**-0.75**	**-0.5**	**-0.25**	**0**	**0.25**	**0.5**	**0.75**	**1**
					$\eta = -3$				
γ_1	0.44210	0.426233	0.41024	0.39413	0.37790	0.36158	0.34519	0.32878	0.31244
γ_2	0.68626	0.669336	0.65217	0.63503	0.61815	0.60177	0.58611	0.57138	0.55777
γ_3	0.81719	0.810279	0.80410	0.79863	0.79385	0.78974	0.78635	0.78369	0.78179
γ_4	1.13133	1.12266	1.11499	1.10833	1.10269	1.09808	1.09451	1.09195	1.09042
γ_5	1.46528	1.45724	1.45006	1.44375	1.43835	1.43384	1.43025	1.42756	1.42578
γ_6	1.8038	1.79663	1.79022	1.78458	1.77971	1.77562	1.77231	1.76978	1.76803
					$\eta = -2$				
γ_1	0.37790	0.361576	0.34519	0.32878	0.31244	0.29626	0.28034	0.26482	0.24983
γ_2	0.61815	0.601766	0.58611	0.57138	0.55777	0.54543	0.53450	0.52507	0.51723
γ_3	0.793849	0.789743	0.78635	0.78369	0.78179	0.78067	0.78038	0.78093	0.78235
γ_4	1.10269	1.09808	1.09451	1.09195	1.09042	1.08988	1.09033	1.09175	1.09412
γ_5	1.43835	1.43384	1.43025	1.42756	1.42578	1.42491	1.42493	1.42585	1.42766
γ_6	1.77971	1.77562	1.77231	1.76978	1.76803	1.76706	1.76687	1.76746	1.76882
					$\eta = -1$				
γ_1	0.31244	0.296257	0.28034	0.26482	0.24983	0.23550	0.22197	0.20933	0.19766
γ_2	0.55777	0.54543	0.53450	0.52507	0.51723	0.51102	0.50647	0.50358	0.50233
γ_3	0.78179	0.780672	0.78038	0.78093	0.78235	0.78466	0.78788	0.79200	0.79702
γ_4	1.09042	1.08988	1.09033	1.09175	1.09412	1.09742	1.10163	1.10673	1.11269
γ_5	1.42578	1.42491	1.42493	1.42585	1.42766	1.43034	1.43388	1.43827	1.4435
γ_6	1.76803	1.76706	1.76687	1.76746	1.76882	1.77095	1.77384	1.77749	1.7819
					$\eta = 0$				
γ_1	0.24983	0.235504	0.22197	0.20933	0.19766	0.18702	0.17741	0.16884	0.16125
γ_2	0.51723	0.511019	0.50647	0.50358	0.50233	0.50268	0.50456	0.50789	0.51258
γ_3	0.78235	0.784662	0.78788	0.79200	0.79702	0.80293	0.80971	0.81733	0.82576
γ_4	1.09412	1.09742	1.10163	1.10673	1.11269	1.11948	1.12709	1.13546	1.14458
γ_5	1.42766	1.43034	1.43388	1.43827	1.4435	1.44954	1.45637	1.46398	1.47234
γ_6	1.76882	1.77095	1.77384	1.77749	1.7819	1.78704	1.79293	1.79953	1.80684
					$\eta = 1$				
γ_1	0.19766	0.187015	0.17741	0.16884	0.16125	0.15458	0.14876	0.14370	0.13930
γ_2	0.50233	0.50268	0.50456	0.50789	0.51258	0.51852	0.52560	0.53369	0.54270
γ_3	0.79702	0.802928	0.80971	0.81733	0.82576	0.83496	0.84487	0.85545	0.86663
γ_4	1.11269	1.11948	1.12709	1.13546	1.14458	1.15441	1.16489	1.176	1.1877
γ_5	1.4435	1.44954	1.45637	1.46398	1.47234	1.48143	1.4912	1.50165	1.51271
γ_6	1.7819	1.78704	1.79293	1.79953	1.80684	1.81486	1.82355	1.8329	1.84289
					$\eta = 2$				
γ_1	0.16125	0.154583	0.14876	0.14370	0.13930	0.13548	0.13217	0.12929	0.12677
γ_2	0.51258	0.518519	0.52560	0.53369	0.54270	0.55249	0.56298	0.57406	0.58565
γ_3	0.82576	0.834957	0.84487	0.85545	0.86663	0.87838	0.89062	0.90331	0.91640
γ_4	1.14458	1.15441	1.16489	1.176	1.1877	1.19992	1.21264	1.2258	1.23936
γ_5	1.47234	1.48143	1.4912	1.50165	1.51271	1.52438	1.53659	1.54932	1.56252
γ_6	1.80684	1.81486	1.82355	1.8329	1.84289	1.85351	1.86471	1.87648	1.88879
					$\eta = 3$				
γ_1	0.13930	0.135483	0.13217	0.12929	0.12677	0.12456	0.12262	0.12090	0.11937
γ_2	0.54270	0.552492	0.56298	0.57406	0.58565	0.59767	0.61005	0.62275	0.63570
γ_3	0.86663	0.878377	0.89062	0.90331	0.91640	0.92983	0.94357	0.95757	0.97178
γ_4	1.1877	1.19992	1.21264	1.2258	1.23936	1.25327	1.2675	1.28201	1.29676
γ_5	1.51271	1.52438	1.53659	1.54932	1.56252	1.57616	1.59019	1.60457	1.61926

Table 5. *Natural frequencies of a fixed-free FGM disk with* $(a/b = 0.1)$ $(\Omega_i = \gamma_i / 0.1, i = 1,2,..,6)$.

m	**-1**	**-0.75**	**-0.5**	**-0.25**	**0**	**0.25**	**0.5**	**0.75**	**1**
					$\eta = -3$				
γ_1	0.44371	0.42830	0.41287	0.39743	0.38198	0.36655	0.35116	0.33582	0.32058
γ_2	0.76918	0.75304	0.73699	0.72107	0.70534	0.68983	0.67461	0.65975	0.64535
γ_3	1.08983	1.07381	1.05804	1.04258	1.02748	1.01281	0.99865	0.98507	0.97214
γ_4	1.41143	1.39618	1.38133	1.36695	1.35308	1.33978	1.3271	1.31511	1.30385
γ_5	1.7361	1.72201	1.70844	1.69541	1.68297	1.67116	1.66001	1.64955	1.63981

m	-1	-0.75	-0.5	-0.25	0	0.25	0.5	0.75	1
γ_6	2.06447	2.05169	2.03947	2.02782	2.01677	2.00634	1.99655	1.98741	1.97894
					$\eta=-2$				
γ_1	0.38198	0.36655	0.35116	0.33582	0.32058	0.30546	0.29053	0.27584	0.26147
γ_2	0.70534	0.68983	0.67461	0.65975	0.64535	0.63149	0.61828	0.60583	0.59426
γ_3	1.02748	1.01281	0.99865	0.98507	0.97214	0.95995	0.94857	0.93807	0.92852
γ_4	1.35308	1.33978	1.3271	1.31511	1.30385	1.29337	1.2837	1.2749	1.26698
γ_5	1.68297	1.67116	1.66001	1.64955	1.63981	1.63081	1.62257	1.61511	1.60846
γ_6	2.01677	2.00634	1.99655	1.98741	1.97894	1.97115	1.96405	1.95764	1.95194
					$\eta=-1$				
γ_1	0.32058	0.30546	0.29053	0.27584	0.26147	0.24748	0.23398	0.22105	0.20879
γ_2	0.64535	0.63149	0.61828	0.60583	0.59426	0.58369	0.57424	0.56603	0.55916
γ_3	0.97214	0.95995	0.94857	0.93807	0.92852	0.92000	0.91256	0.90626	0.90113
γ_4	1.30385	1.29337	1.2837	1.2749	1.26698	1.26	1.25397	1.24891	1.24484
γ_5	1.63981	1.63081	1.62257	1.61511	1.60846	1.60261	1.59759	1.5934	1.59006
γ_6	1.97894	1.97115	1.96405	1.95764	1.95194	1.94695	1.94267	1.93912	1.93629
					$\eta=0$				
γ_1	0.26147	0.24748	0.23398	0.22105	0.20879	0.19730	0.18665	0.17689	0.16808
γ_2	0.59426	0.58369	0.57424	0.56603	0.55916	0.55373	0.54981	0.54745	0.54669
γ_3	0.92852	0.92000	0.91256	0.90626	0.90113	0.89721	0.89454	0.89313	0.89299
γ_4	1.26698	1.26	1.25397	1.24891	1.24484	1.24179	1.23975	1.23874	1.23877
γ_5	1.60846	1.60261	1.59759	1.5934	1.59006	1.58756	1.58592	1.58514	1.58521
γ_6	1.95194	1.94695	1.94267	1.93912	1.93629	1.93419	1.93281	1.93217	1.93226
					$\eta=1$				
γ_1	0.20879	0.19730	0.18665	0.17689	0.16808	0.16022	0.15328	0.14723	0.14199
γ_2	0.55916	0.55373	0.54981	0.54745	0.54669	0.54750	0.54987	0.55373	0.55900
γ_3	0.90113	0.89721	0.89454	0.89313	0.89299	0.89412	0.89651	0.90013	0.90496
γ_4	1.24484	1.24179	1.23975	1.23874	1.23877	1.23983	1.24191	1.24502	1.24914
γ_5	1.59006	1.58756	1.58592	1.58514	1.58521	1.58615	1.58795	1.5906	1.59411
γ_6	1.93629	1.93419	1.93281	1.93217	1.93226	1.93309	1.93465	1.93694	1.93997
					$\eta=2$				
γ_1	0.16808	0.16022	0.15328	0.14723	0.14199	0.13749	0.13364	0.13033	0.12750
γ_2	0.54669	0.54750	0.54987	0.55373	0.55900	0.56558	0.57334	0.58215	0.59188
γ_3	0.89299	0.89412	0.89651	0.90013	0.90496	0.91094	0.91802	0.92615	0.93524
γ_4	1.23877	1.23983	1.24191	1.24502	1.24914	1.25425	1.26033	1.26735	1.27528
γ_5	1.58521	1.58615	1.58795	1.5906	1.59411	1.59847	1.60366	1.60968	1.61652
γ_6	1.93226	1.93309	1.93465	1.93694	1.93997	1.94372	1.9482	1.95341	1.95934
					$\eta=3$				
γ_1	0.14199	0.13749	0.13364	0.13033	0.12750	0.12507	0.12296	0.12113	0.11952
γ_2	0.55900	0.56558	0.57334	0.58215	0.59188	0.60242	0.61363	0.62541	0.63766
γ_3	0.90496	0.91094	0.91802	0.92615	0.93524	0.94523	0.95602	0.96754	0.97969
γ_4	1.24914	1.25425	1.26033	1.26735	1.27528	1.28408	1.29371	1.30412	1.31525
γ_5	1.59411	1.59847	1.60366	1.60968	1.61652	1.62415	1.63256	1.64172	1.65161

Table 6. *Natural frequencies of a fixed-fixed FGM disk with* $(a/b=0.1)$ $(\Omega_i=\gamma_i/0.1,\ i=1,2,..,6)$.

m	-1	-0.75	-0.5	-0.25	0	0.25	0.5	0.75	1
					$\eta=-3$				
γ_1	0.57525	0.560977	0.54680	0.53276	0.51887	0.50520	0.49178	0.47870	0.46603
γ_2	0.90936	0.894285	0.87941	0.86480	0.85049	0.83655	0.82307	0.81013	0.79781
γ_3	1.2354	1.22054	1.20604	1.19195	1.17833	1.16525	1.15279	1.141	1.12995
γ_4	1.5614	1.54739	1.53386	1.52086	1.50845	1.49667	1.48557	1.47518	1.46554
γ_5	1.88986	1.87701	1.86473	1.85302	1.84193	1.83149	1.82172	1.81263	1.80426
γ_6	2.22145	2.20984	2.1988	2.18835	2.1785	2.16926	2.16065	2.15268	2.14536
					$\eta=-2$				
γ_1	0.51887	0.505197	0.49178	0.47870	0.46603	0.45388	0.44234	0.43156	0.42168
γ_2	0.85049	0.836553	0.82307	0.81013	0.79781	0.78621	0.77543	0.76556	0.75671
γ_3	1.17833	1.16525	1.15279	1.141	1.12995	1.11971	1.11034	1.10188	1.09439
γ_4	1.50845	1.49667	1.48557	1.47518	1.46554	1.4567	1.44867	1.44148	1.43516
γ_5	1.84193	1.83149	1.82172	1.81263	1.80426	1.79661	1.78971	1.78355	1.77816

m	**-1**	**-0.75**	**-0.5**	**-0.25**	**0**	**0.25**	**0.5**	**0.75**	**1**
γ_6	2.1785	2.16926	2.16065	2.15268	2.14536	2.13869	2.13269	2.12734	2.12267
					$\eta=-1$				
γ_1	0.46603	0.453876	0.44234	0.43156	0.42168	0.41284	0.40520	0.39890	0.39409
γ_2	0.79781	0.78621	0.77543	0.76556	0.75671	0.74896	0.74238	0.73706	0.73306
γ_3	1.12995	1.11971	1.11034	1.10188	1.09439	1.0879	1.08246	1.0781	1.07484
γ_4	1.46554	1.4567	1.44867	1.44148	1.43516	1.42973	1.42519	1.42157	1.41886
γ_5	1.80426	1.79661	1.78971	1.78355	1.77816	1.77353	1.76968	1.76662	1.76433
γ_6	2.14536	2.13869	2.13269	2.12734	2.12267	2.11867	2.11535	2.1127	2.11073
					$\eta=0$				
γ_1	0.42168	0.412837	0.40520	0.39890	0.39409	0.39088	0.38934	0.38951	0.39139
γ_2	0.75671	0.748955	0.74238	0.73706	0.73306	0.73041	0.72915	0.72929	0.73083
γ_3	1.09439	1.0879	1.08246	1.0781	1.07484	1.07269	1.07167	1.07178	1.07303
γ_4	1.43516	1.42973	1.42519	1.42157	1.41886	1.41709	1.41625	1.41634	1.41737
γ_5	1.77816	1.77353	1.76968	1.76662	1.76433	1.76283	1.76212	1.7622	1.76307
γ_6	2.12267	2.11867	2.11535	2.1127	2.11073	2.10944	2.10883	2.1089	2.10964
					$\eta=1$				
γ_1	0.39409	0.39088	0.38934	0.38951	0.39139	0.39493	0.40005	0.40662	0.41451
γ_2	0.73306	0.730408	0.72915	0.72929	0.73083	0.73375	0.73802	0.74360	0.75041
γ_3	1.07484	1.07269	1.07167	1.07178	1.07303	1.0754	1.07889	1.08347	1.08912
γ_4	1.41886	1.41709	1.41625	1.41634	1.41737	1.41933	1.42222	1.42602	1.43074
γ_5	1.76433	1.76283	1.76212	1.7622	1.76307	1.76472	1.76717	1.77039	1.7744
γ_6	2.11073	2.10944	2.10883	2.1089	2.10964	2.11107	2.11318	2.11596	2.11942
					$\eta=2$				
γ_1	0.39139	0.394932	0.40005	0.40662	0.41451	0.42358	0.43365	0.44459	0.45626
γ_2	0.73083	0.733751	0.73802	0.74360	0.75041	0.75840	0.76746	0.77752	0.78847
γ_3	1.07303	1.0754	1.07889	1.08347	1.08912	1.0958	1.10349	1.11214	1.12169
γ_4	1.41737	1.41933	1.42222	1.42602	1.43074	1.43635	1.44285	1.45021	1.4584
γ_5	1.76307	1.76472	1.76717	1.77039	1.7744	1.77918	1.78472	1.79103	1.79808
γ_6	2.10964	2.11107	2.11318	2.11596	2.11942	2.12355	2.12836	2.13383	2.13997
					$\eta=3$				
γ_1	0.41451	0.423576	0.43365	0.44459	0.45626	0.46853	0.48129	0.49444	0.50791
γ_2	0.75041	0.758395	0.76746	0.77752	0.78847	0.80022	0.81267	0.82573	0.83931
γ_3	1.08912	1.0958	1.10349	1.11214	1.12169	1.1321	1.1433	1.15523	1.16782
γ_4	1.43074	1.43635	1.44285	1.45021	1.4584	1.46741	1.4772	1.48773	1.49898
γ_5	1.7744	1.77918	1.78472	1.79103	1.79808	1.80588	1.81439	1.82362	1.83353

Table 7. *Variation of the first three natural frequencies with the profile parameter, inhomogeneity index, and boundary conditions of a FGM disk with* $(a/b=0.5)$ $(\Omega_i=\gamma_i/0.5,\ i=1,2,3)$.

m	**-1**	**-0.75**	**-0.5**	**-0.25**	**0**	**0.25**	**0.5**	**0.75**	**1**
	$a/b=0.5$ free-free								
	$\eta=-3$								
γ_1	0.76651	0.76056	0.75447	0.74824	0.74188	0.73541	0.72883	0.72218	0.71548
γ_2	3.30919	3.28823	3.26935	3.2526	3.23801	3.22561	3.21542	3.20746	3.20175
γ_3	6.37388	6.36209	6.35149	6.34209	6.33387	6.32686	6.32106	6.31646	6.31307
					$\eta=0$				
γ_1	0.68830	0.68154	0.67482	0.66818	0.66163	0.65517	0.64884	0.64264	0.63659
γ_2	3.20146	3.20701	3.21479	3.22476	3.23692	3.25123	3.26765	3.28615	3.3067
γ_3	6.31162	6.31429	6.31817	6.32326	6.32955	6.33704	6.34573	6.35561	6.36668
					$\eta=3$				
γ_1	0.61405	0.60887	0.60387	0.59907	0.59446	0.59003	0.58580	0.58175	0.57788
γ_2	3.4084	3.43847	3.47029	3.50382	3.539	3.57577	3.61408	3.65388	3.69512
γ_3	6.4227	6.43961	6.45765	6.47684	6.49714	6.51856	6.54109	6.56471	6.58941
	$a/b=0.5$ fixed-free								
	$\eta=-3$								
γ_1	2.4934	2.4319	2.37095	2.31059	2.25083	2.19171	2.13325	2.07549	2.01844
γ_2	5.17293	5.13614	5.10043	5.06584	5.03238	5.00008	4.96898	4.93908	4.91043
γ_3	8.14697	8.12272	8.09931	8.07676	8.05507	8.03424	8.01429	7.99523	7.97706
	$\eta=0$								
γ_1	1.79808	1.7451	1.69302	1.64188	1.59171	1.54254	1.4944	1.44733	1.40134

m	-1	-0.75	-0.5	-0.25	0	0.25	0.5	0.75	1
γ_2	4.80878	4.78674	4.7661	4.74689	4.72914	4.71286	4.69809	4.68485	4.67317
γ_3	7.91345	7.89986	7.8872	7.87548	7.86471	7.8549	7.84604	7.83816	7.83124
					$\eta = 3$				
γ_1	1.22894	1.18885	1.15002	1.11246	1.07621	1.04126	1.00764	0.97536	0.94443
γ_2	4.64237	4.63876	4.63681	4.63654	4.63796	4.64109	4.64593	4.65248	4.66075
γ_3	7.81339	7.81141	7.81042	7.81043	7.81145	7.81347	7.8165	7.82053	7.82558
	$a/b = 0.5$ fixed-fixed								
	$\eta = -3$								
γ_1	3.55255	3.51615	3.4814	3.44836	3.41707	3.38759	3.35999	3.3343	3.31058
γ_2	6.51118	6.49007	6.47008	6.45121	6.43349	6.41691	6.40149	6.38723	6.37415
γ_3	9.57998	9.56548	9.55178	9.53887	9.52676	9.51545	9.50494	9.49524	9.48634
	$\eta = 0$								
γ_1	3.23626	3.22302	3.21197	3.20315	3.19658	3.19226	3.19022	3.19044	3.19294
γ_2	6.33366	6.32652	6.32059	6.31586	6.31235	6.31005	6.30895	6.30907	6.31041
γ_3	9.45888	9.45405	9.45004	9.44684	9.44446	9.44291	9.44217	9.44225	9.44315
	$\eta = 3$								
γ_1	3.22549	3.23917	3.25501	3.27298	3.29305	3.31516	3.33928	3.36536	3.39334
γ_2	6.32785	6.33523	6.3438	6.35357	6.36453	6.37667	6.38999	6.40448	6.42013
γ_3	9.45495	9.45994	9.46575	9.47237	9.47981	9.48806	9.49711	9.50698	9.51764

Table 8. *Variation of the first three natural frequencies with the profile parameter, inhomogeneity index, and boundary conditions of a FGM disk with* $(a/b = 0.9)$ $(\Omega_i = \gamma_i / 0.9,\ i = 1,2,3)$.

m	-1	-0.75	-0.5	-0.25	0	0.25	0.5	0.75	1
	$a/b = 0.9$ free-free								
	$\eta = -3$								
γ_1	0.90100	0.90779	0.90758	0.90737	0.90716	0.90695	0.90674	0.90653	0.90632
γ_2	28.3116	28.3067	28.3023	28.2984	28.295	28.2921	28.2896	28.2877	28.2863
γ_3	56.5674	56.5649	56.5627	56.5607	56.559	56.5575	56.5563	56.5554	56.5546
	$\eta = 0$								
γ_1	0.90549	0.90528	0.90507	0.90486	0.90465	0.90444	0.90423	0.90402	0.90381
γ_2	28.2855	28.2865	28.2881	28.2901	28.2927	28.2957	28.2992	28.3032	28.3078
γ_3	56.5542	56.5548	56.5555	56.5566	56.5578	56.5593	56.5611	56.5631	56.5654
	$\eta = 3$								
γ_1	0.90298	0.90277	0.90256	0.90236	0.90215	0.90194	0.90174	0.90153	0.90132
γ_2	28.3308	28.3378	28.3452	28.3532	28.3617	28.3707	28.3801	28.3901	28.4005
γ_3	56.5769	56.5804	56.5842	56.5882	56.5924	56.5969	56.6017	56.6066	56.6119
	$a/b = 0.9$ fixed-free								
	$\eta = -3$								
γ_1	15.2682	15.1904	15.1127	15.0352	14.9579	14.8808	14.8039	14.7271	14.6505
γ_2	42.8146	42.7853	42.7563	42.7276	42.6992	42.6711	42.6432	42.6157	42.5884
γ_3	70.9291	70.9114	70.8938	70.8764	70.8592	70.8422	70.8254	70.8087	70.7923
	$\eta = 0$								
γ_1	14.3461	14.2705	14.195	14.1197	14.0447	13.9698	13.8951	13.8206	13.7463
γ_2	42.4824	42.4567	42.4312	42.4061	42.3812	42.3566	42.3324	42.3085	42.2848
γ_3	70.7285	70.713	70.6977	70.6826	70.6677	70.653	70.6384	70.6241	70.61
					$\eta = 3$				
γ_1	13.451	13.3776	13.3045	13.2315	13.1588	13.0862	13.0139	12.9417	12.8698
γ_2	42.1933	42.1712	42.1494	42.128	42.1068	42.086	42.0654	42.0452	42.0253
γ_3	70.5554	70.5422	70.5293	70.5165	70.5039	70.4915	70.4793	70.4673	70.4555
	$a/b = 0.9$ fixed-fixed								
	$\eta = -3$								
γ_1	28.3687	28.3599	28.3515	28.3436	28.3362	28.3293	28.323	28.3171	28.3116
γ_2	56.596	56.5915	56.5873	56.5834	56.5797	56.5762	56.573	56.5701	56.5674
γ_3	84.8546	84.8516	84.8488	84.8462	84.8437	84.8414	84.8392	84.8373	84.8355
	$\eta = 0$								
γ_1	28.295	28.2921	28.2896	28.2877	28.2862	28.2853	28.2849	28.2849	28.2855
γ_2	56.559	56.5575	56.5563	56.5554	56.5546	56.5542	56.5539	56.554	56.5542
γ_3	84.8299	84.8289	84.8281	84.8275	84.827	84.8267	84.8265	84.8265	84.8267
	$\eta = 3$								

m	**-1**	**-0.75**	**-0.5**	**-0.25**	**0**	**0.25**	**0.5**	**0.75**	**1**
γ_1	28.2926	28.2956	28.2991	28.3032	28.3077	28.3127	28.3182	28.3242	28.3307
γ_2	56.5578	56.5593	56.5611	56.5631	56.5654	56.5679	56.5706	56.5736	56.5769
γ_3	84.8291	84.8301	84.8313	84.8326	84.8341	84.8358	84.8377	84.8397	84.8418

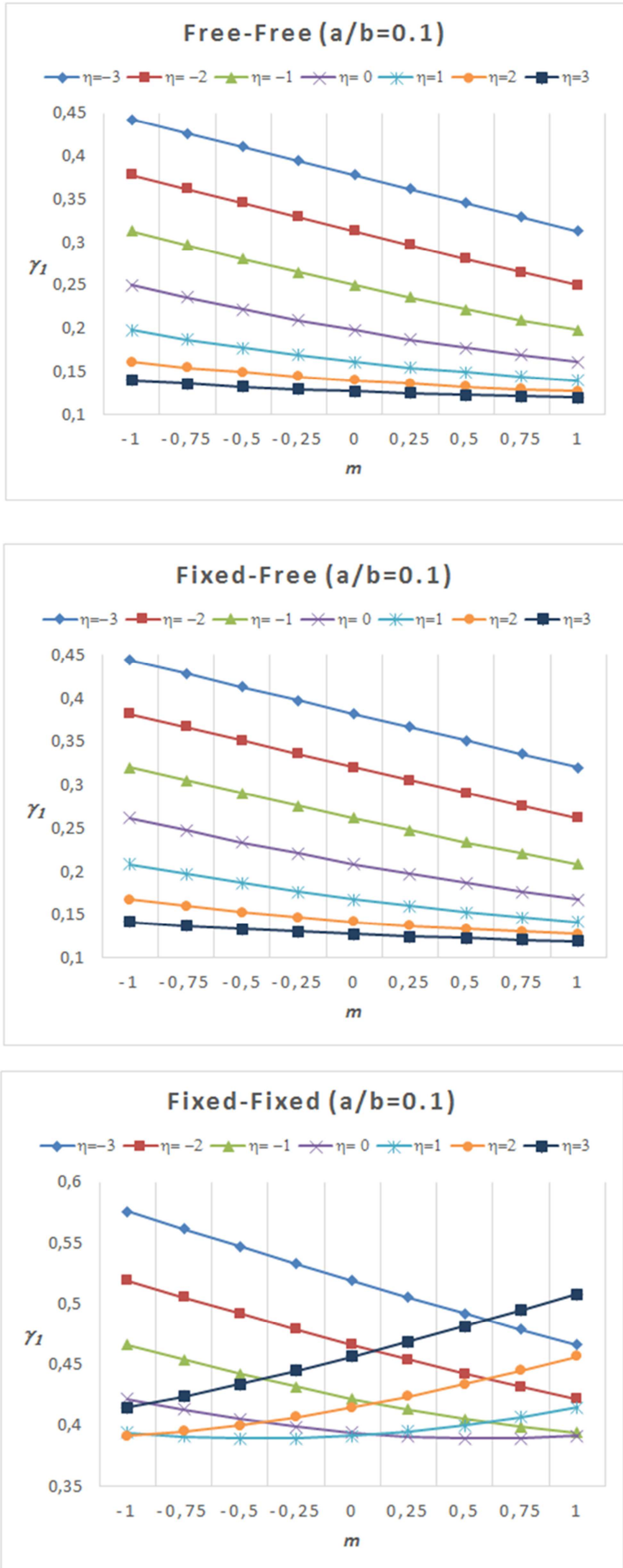

(a) $a/b=0.1$

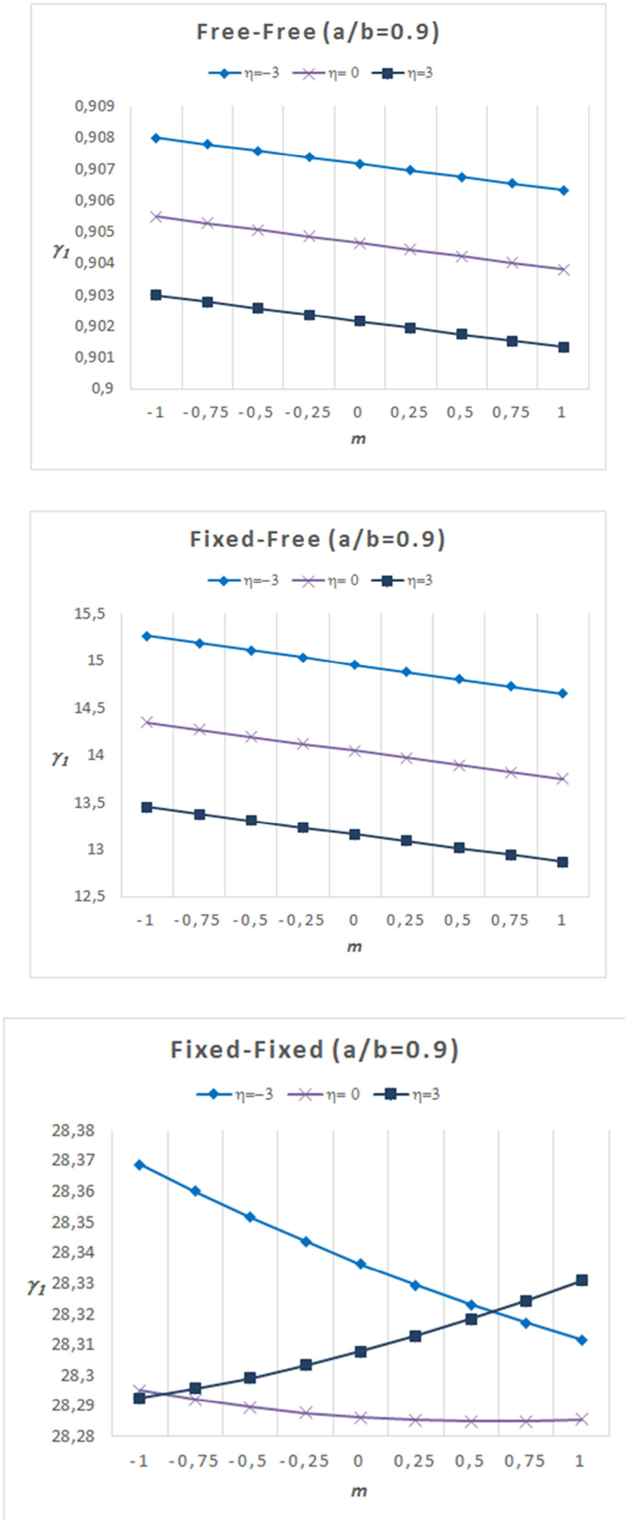

(b) $a/b=0.9$

Figure 5. *Variation of the fundamental dimensionless frequencies with the profile parameter, inhomogeneity index, and boundary conditions.*

References

[1] Leissa, A. W., 1978, “Recent research in plate vibration, 1973–1976: Complicating effects,” Shock Vib Dig, Vol. 10, pp. 21–35.

[2] Leissa, A. W., 1981, “Plate vibration research, 1976–1980: Classical theory,” The Shock and Vibration Digest, Vol. 13, pp. 11-22.

[3] Leissa, A. W., 1981, “Plate vibration research, 1976–1980: Complicating effects,” Shock Vib Dig, Vol. 13, pp. 19–36.

[4] Leissa, A. W., 1987, “Recent studies in plate vibrations, 1981–1985: Part II-–Complicating effects,” Shock Vib Dig, Vol. 19, pp. 10–24.

[5] Leissa, A. W., 1987, “Recent studies in plate vibrations: 1981–1985, Part I: Classical theory,” The Shock and Vibration Digest, Vol. 19, pp. 11-18.

[6] Swaminathan, K., Naveenkumar D. T., Zenkour A. M., Carrera E., 2015, “Stress, vibration and buckling analyses of FGM plates-A state-of-the-art review,” Compos Struct, Vol. 120, pp. 10-31.

[7] Brunelle, E. J., 1970, “Stress redistribution and instability of rotating beams and disks,” AIAA Journal, Vol. 9 (4), pp. 758-759.

[8] Ambati, G., Bell J. F. W., Sharp, J. C. K., 1976, “In-plane vibrations of annular rings,” Journal of Sound and Vibration, Vol. 47 (3), pp. 415–432.

[9] Irie, T., Yamada, G., Muramoto, Y., 1984, “Natural frequencies of in-plane vibration of annular plates,” Journal of Sound and Vibration, Vol. 97 (1), pp. 171–175.

[10] Chen, J. S., Jhu, J. L., 1996, “On the in-plane vibration and stability of a spinning annular disk,” Journal of Sound and Vibration, Vol. 195 (4), pp. 585–593.

[11] Tzou, K. I., Wickert, J. A., Akay, A., 1998, “In-plane vibration modes of arbitrarily thick disks,” Journal of Vibration and Acoustics, Vol. 120 (2), pp. 384–391.

[12] Zhou, D., Au, F. T. K., Cheung, Y. K., Lo, S. H., 2003, “Three dimensional vibration analysis of circular and annular plates via the Chebyshev-Ritz method,” International Journal of Solids and Structures, Vol. 40, 3089–3105.

[13] Civalek, O, 2008, “Discrete singular convolution method and applications to free vibration analysis of circular and annular plates,” Structural Engineering and Mechanics, Vol. 29 (2), pp. 237–240.

[14] Dong, C. Y., 2008, “Three-dimensional free vibration analysis of functionally graded annular plates using the Chebyshev–Ritz method,” Mater Des, Vol. 29 (8), pp. 1518–1525.

[15] Bashmal, S., Bhat, R., Rakheja, S., 2009, “In-plane free vibration of circular annular disks,” Journal of Sound and Vibration, Vol. 322, pp. 216–226.

[16] Bashmal, S., Bhat, R., Rakheja, S., 2010, “Frequency equations for the in-plane vibration of circular annular disks,” Advances in Acoustics and Vibration, Article ID 501902, 8 pages, doi: 10.1155/2010/501902

[17] Bashmal S., Bhat, R., Rakheja, S., 2011, “In-plane free vibration analysis of an annular disk with point elastic support,” Shock and Vibration, Vol. 18, pp. 627–640, DOI 10.3233/SAV-2010-0578.

[18] Carrera, E., Filippi, M., Zappino, 2013, E. “Free vibration analysis of rotating structures by one-dimensional, variable kinematic theories,” ASME 2013 International Mechanical Engineering Congress and Exposition, Volume 9: Mechanics of Solids, Structures and Fluids, San Diego, California, USA, November 15–21, 2013, Paper No. IMECE2013-63183, pp. V009T10A021; 10 pages, doi: 10.1115/IMECE2013-63183

[19] Squarcella, N., Firrone, C. M., Allara, M., Gola, Muzio, 2014, “The importance of the material properties on the burst speed of turbine disks for aeronautical applications,” Int J Mech Sci, Vol. 84, pp. 73-83.

[20] Duan, G., Wang, X., Jin, C., 2014, “Free vibration analysis of circular thin plates with stepped thickness by the DSC element method,” Thin Walled Struct, Vol. 85, pp. 25-33.

[21] Mercan K., Ersoy H., Civalek, O, 2016, “Free vibration of annular plates by discrete singular convolution and differential quadrature methods,” Journal of Applied and Computational Mechanics, Vol. 2 (3), pp. 128-133.

[22] Ramaiah, G. K., Vijaykumar, K., 1975, “Vibrations of annular plates with linear thickness profiles,” J Sound Vib, Vol. 40, pp. 293–298.

[23] Sato, H., Shimizu C., 1984, “Transfer matrix analysis of non-linear free vibrations of circular plates with variable thickness,” Journal of Sound and Vibration, Vol. 97 (4), pp. 587-595.

[24] Shahab, A., 1993, “Finite element analysis for the vibration of variable thickness discs,” Journal of Sound and Vibration, Vol. 162, pp. 67–88.

[25] Singh, B., Chakraverty, S., 1994, “Use of characteristic orthogonal polynomials in two dimensions for the transverse vibration of elliptical and circular plates with variable thickness,” J Sound Vib, Vol. 173, pp. 289–99.

[26] Singh, B., Saxena, V., 1996, “Axisymmetric vibration of a circular plate with exponential thickness variation,” J Sound Vib, Vol. 192, pp. 35-42.

[27] Wang X., Yang, J., Xiao, J., “On free vibration analysis of circular annular plates with non-uniform thickness by the differential quadrature method,” J Sound Vib, Vol. 184, pp. 547-551.

[28] Laura, P. A. A., Avalos, D. R., Larrondo, H. A., Sonzogni, V., 1996, “Comments on free vibration analysis of circular and annular plates with non-uniform thickness by the differential quadrature method,” Journal of Sound and Vibration, Vol. 195, pp. 338-339.

[29] Wang, J., 1997, “Generalized power series solutions of the vibration of classical circular plates with variable thickness,” J Sound Vib, Vol. 202 (4), pp. 593–599.

[30] Singh, B., Hassan, S. M., 1998, “Transverse vibration of a circular plate with arbitrary thickness variation,” Int J Mech Sci, Vol. 40 (11), pp. 1089–1104.

[31] Ye, Z., 1999, “Application of Maple V to the nonlinear vibration analysis of circular plate with variable thickness,” Comput Struct, Vol. 71, pp. 481–488.

[32] Kang, J. H., Leissa, A. W., 1998, “Three-dimensional vibrations of thick, linearly tapered, annular plates,” J Sound Vib, Vol. 217 (5), pp. 927–944.

[33] Salmane, A., Lakis, A. A., 1999, "Natural frequencies of transverse vibrations of non-uniform circular and annular plates," Journal of Sound and Vibration, Vol. 220, pp. 225-249.

[34] Eisenberger M., Jabareen, M., 2001, "Axisymmetric vibrations of circular and annular plates with variable thickness," International Journal of Structural Stability and Dynamics, Vol. 1 (2), pp. 195-206.

[35] Wu, T. Y., Liu, G. R., 2001, "Free vibration analysis of circular plates with variable thickness by the generalized differential quadrature rule," International Journal of Solids and Structures, Vol. 38 (44), pp. 7967-7980.

[36] Kang, J. H., 2003, "Three-dimensional vibration analysis of thick, circular and annular plates with nonlinear thickness variation," Computers and Structures, Vol. 81, pp. 1663–1675.

[37] Duan, W. H., Quek, S. T., Wang, Q., 2005, "Generalized hypergeometric function solutions for transverse vibration of a class of non-uniform annular plates," Journal of Sound and Vibration, Vol. 287, pp. 785-807.

[38] Alipour, M. M., Shariyat, M., 2011, "Semi-analytical buckling analysis of heterogeneous variable thickness viscoelastic circular plates on elastic foundations," Mechanics Research Communications, Vol. 38 (8), pp. 594-601.

[39] Bhardwaj, N., Gupta, A. P., Choong, K. K., 2008, "Asymmetric vibration of polar orthotropic annular circular plates of quadratically varying thickness with same boundary conditions," Shock and Vibration, Vol. 15 (6), pp. 599-617.

[40] Güven U., Çelik A., 2001, "On transverse vibrations of functionally graded isotropic linearly elastic rotating solid disks," Mechanics Research Communications, 28 (3), Vol. pp. 271-276.

[41] Nie G. J., Zhong Z., 2007, "Semi-analytical solution for three-dimensional vibration of functionally graded circular plates," Journal of Computer Method in Applied Mechanics and Engineering, 196 (49-52), Vol. pp. 4901–4910.

[42] Efraim, E., Eisenberger, M., 2007, "Exact vibration analysis of variable thickness thick annular isotropic and FGM plates," Journal of Sound and Vibration, Vol. 299 (4–5), pp. 720-738.

[43] Allahverdizadeh, A., Naei, M. H., Bahrami, M. N., 2008, "Nonlinear free and forced vibration analysis of thin circular functionally graded plates," J Sound Vib, Vol. 310 (4-5), pp. 966-984.

[44] Dong, C. Y., 2008, "Three-dimensional free vibration analysis of functionally graded annular plates using the Chebyshev-Ritz method," Materials & Design, Vol. 29 (8), pp. 1518-1525.

[45] Prakash, T., Ganapathi, M., 2006, "Asymmetric flexural vibration and thermoelastic stability of FGM circular plates using finite element method," Composites Part B, Vol. 37, pp. 642–649.

[46] Ramirez, F., Heyliger, P. R., Pan, E., 2006, "Discrete layer solution to free vibrations of functionally graded magneto-electro-elastic plates," Mechanics of Advanced Materials and Structures, Vol. 13, pp. 249–266.

[47] Tornabene, F., Viola, E., Inman, D. J., 2009, "2-D differential quadrature solution for vibration analysis of functionally graded conical, cylindrical shell and annular plate structures," J Sound Vib, Vol. 328, pp. 259-290.

[48] Hosseini-Hashemi, S., Fadaee, M., Es'haghi, M., 2010, "A novel approach for in-plane/out-of-plane frequency analysis of functionally graded circular/annular plates," Int J Mech Sci, Vol. 52 (8), pp. 1025–35.

[49] Malekzadeh, P., Shahpari, S. A., Ziaee, H. R., 2010, "Three-dimensional free vibration of thick functionally graded annular plates in thermal environment," J Sound Vib, Vol. 329 (4), pp. 425–442.

[50] Keleş İ., Tütüncü N., 2011, "Exact analysis of axisymmetric dynamic response of functionally graded cylinders (or disks) and spheres," Journal of Applied Mechanics, Vol. 78 (6), 061014 (7 pages).

[51] Tajeddini, V., Ohadi, A., 2011, "Three-dimensional vibration analysis of functionally graded thick, annular plates with variable thickness via polynomial-Ritz method," Journal of Vibration and Control, Vol. 18 (11), pp. 1698–1707. DOI: 10.1177/10775463114037891077546311403789.

[52] Shamekhi, A., 2013, "On the use of meshless method for free vibration analysis of circular FGM plate having variable thickness under axisymmetric condition," International Journal of Research and Reviews in Applied Sciences, Vol. 14 (2), pp. 257-268.

[53] Lhoucine, B., Khalid, E. B., Rhali, B., 2014, "Large amplitude free vibration analysis of functionally graded annular plates," Adv Mater Res, Vol. 971, pp. 548-564.

[54] Çallıoğlu, H., Demir, E., Yılmaz, Y., Girgin, Z., 2014, "Vibration behavior of a radially functionally graded annular disc with variable geometry," Sci Eng Compos Mater, Vol. 21 (3), pp. 453–461.

[55] Ravaei, M., Nahvi, H., 2014, "Disk vibration analysis of functionally graded materials," Journal of Solid Mechanics in Engineering, Vol. 7: 2 (16), pp. 29-35.

[56] Lal, R., Ahlawat, N., 2015, "Buckling and Vibration of Functionally Graded Non-uniform Circular Plates Resting on Winkler Foundation," Latin American Journal of Solids and Structures, Vol. 12, 2015, pp. 2231-2258.

[57] Torabi, J., Ansari, R., 2017, "Nonlinear free vibration analysis of thermally induced FG-CNTRC annular plates: Asymmetric versus axisymmetric study," Computer Methods in Applied Mechanics and Engineering, Vol. 324 (1), pp. 327-347.

[58] Yang, Y., Kou, K. P., Lam, C. C., 2017, "In-plane free vibration of circular and annular FG disks," The 8th International Conference on Computational Methods (ICCM2017), July 25-29th, Guilin, Guangxi, China, http://www.sci-en-tech.com/ICCM2017/PDFs/2627-9022-1-PB.pdf, pp. 1-11.

[59] Mahinzare, M., Ranjbarpur, H., Ghadiri, M., 2018, "Free vibration analysis of a rotary smart two directional functionally graded piezoelectric material in axial symmetry circular nanoplate," Mechanical Systems and Signal Processing, Vol. 100, pp. 188–207.

[60] Abramowitz, M., Stegun, I. A., Handbook of Mathematical Functions with Formulas, Graphs and Mathematical Tables. 9th printing, New York, Dover, 1972.